Quantitative Economics 13 (2022), 225–257 1759-7331/20220225

Modeling time varying risk of natural resource assets: Implications of climate change

Anke D. Leroux
Department of Economics, Monash University

Vance L. Martin
Department of Economics, University of Melbourne

Kathryn A. St. John
Department of Economics, University of Melbourne

A multivariate GARCH model of natural resources is specified to capture the effects of time varying portfolio risk. A special feature of the model is the inclusion of realized volatility for natural resource assets that are available at multiple frequencies as well as being sensitive to sudden changes in climatic conditions. Natural resource portfolios under climate change are simulated from bootstrapping schemes as well as being derived from global climate model projections. Both approaches are applied to a multiasset water portfolio model consisting of reservoir inflows, rainwater harvesting, and desalinated water. The empirical results show that while reservoirs remain the dominant water asset, adaptation to climate change involves increased contributions from rainwater harvesting and more frequent use of desalinated water. It is estimated that climate change increases annual water supply costs by between 7% and 44% over a 20-year forecast horizon.

Keywords. RV-DCC, realized variance, natural resource portfolio, climate change.
JEL classification. C32, C53, Q35, Q54.

1. Introduction

Understanding risk is important in constructing optimal portfolios of financial (Merton (1969)) as well as natural assets. In the latter case, examples include the optimal composition of energy (Humphreys and McClain (1998)), water (Leroux and Martin (2016),

Anke D. Leroux: anke.leroux@monash.edu
Vance L. Martin: vance@unimelb.edu.au
Kathryn A. St. John: stjohnka@gmail.com
The authors would like to thank two anonymous referees for their insightful and constructive comments. We give our special thanks to Murray Peel for his help in generating local reservoir and rainwater harvesting projections for each of the RCP scenarios. The authors would like to thank Mindy Mallory for her suggestions on an earlier draft of the paper and seminar participants at ESAM18 in Auckland, the 2018 NCER conference in Brisbane, the Econometric workshop in Jyväskylä in April 2018, the 2018 Monash Environmental Economics Workshop in Melbourne, the 2019 AERE Summer Conference at Lake Tahoe, and the 2019 AAEA Meeting in Atlanta. Funding from the ARC, Grant DP140102137 and the CRC for Water Sensitive Cities, Grant 2014001467 is gratefully acknowledged.

 https://doi.org/10.3982/QE1597

Leroux, Martin, and Zheng (2018)), fisheries (Sanchirico, Smith, and Lipton (2008)), and habitat portfolios (Ando and Mallory (2012), Mallory and Ando (2014), Shah and Ando (2015), Duran Vinent, Johnston, Kirwan, Leroux, and Martin (2019)) to assure supply or conservation objectives. Time variations in risks and corisks require frequent rebalancing of portfolios, which is common practice in financial asset portfolios (Baillie and Myers (1991) and Tischbirek (2019)), but is less common in the case of natural asset portfolios.[1] Yet, the efficient rebalancing of portfolios involving climate dependent assets is essential to achieving least cost adaptation in the face of accelerating climatic change (Stocker et al. (2014), WWAP (2012)).

The aim of this paper is to propose a framework that circumvents the restriction of constant volatility risk, imposed by previous approaches to modeling natural assets. To capture the effects of time varying climate risks on natural assets, a multivariate class of volatility models is specified based on augmenting the dynamic conditional correlation (DCC) model of Engle (2002) with the realized GARCH volatility (RV GARCH) model of Hansen, Lunde, and Voev (2012).[2] The DCC component of the model captures the time variations in the corisks of the natural assets, thereby allowing for time variations in the resource portfolios. This class of models is referred to as the RV DCC model. There are two reasons for augmenting the DCC model by realized volatility. First, when data are available at multiple frequencies for some, but not necessarily all natural assets, realized volatility measures provide a framework for combining all available information to improve the precision of the time varying estimates of risk. Second, realized measures of volatility are known to be more effective in capturing rapid movements in the underlying latent volatility process than standard GARCH models (Hansen, Lunde, and Voev (2012)). This is especially important in modeling natural resources that are affected by sudden changes in climatic conditions.

The RV DCC model is applied to modeling a set of water supply assets consisting of two climate sensitive water assets, reservoirs, and rainwater harvesting, as well as a risk-free asset based on desalinated water.[3] Using nearly 100 years of monthly data for Melbourne, Australia, the empirical results provide strong evidence of time variations in volatility risk and corisks of the water assets. Realized volatility estimates based on the availability of higher frequency data for harvested water are found to help predict future movements in volatility of the water assets.

The estimated empirical model is used to construct optimal water supply portfolios under various climate conditions and scenarios for the water assets.[4] Under historical

[1] An exception is Humphreys and McClain (1998), who adopt a conventional financial framework based on energy assets.

[2] For a review of multivariate GARCH models, see Bauwens, Laurent, and Rombouts (2006).

[3] Water rights are well-defined in Australia and water assets are typically owned and managed by a combination of government, government agencies as well as private partners. Melbourne Water is the statutory authority owned by the Victorian government that is tasked with overseeing and protecting Melbourne's water supply and water assets. The term rainwater harvesting as used in this paper refers to the harvesting of urban rain and storm water in small-scale, decentralized systems that are designed to capture urban runoff from impermeable surfaces in rainwater tanks, ponds, urban wetlands, and swales (Ahammed (2017)) and is distinct from capturing water in large-scale, centralized reservoirs.

[4] Following Merton (1969, 1971), an optimal portfolio jointly optimizes the consumption path from a portfolio of assets with stochastic returns and the composition (asset shares) of the portfolio over time.

conditions, the major contribution to the optimal water portfolio is from reservoirs, with the remainder coming from rainwater harvesting and desalination. While rainwater harvesting contributes almost continuously to the water stock, the contributions from desalination are infrequent under normal conditions and increasing to around 25% of the time under recent millennium drought conditions.[5] The effects of climate change on the future water portfolio are captured by adopting two bootstrapping schemes. The first involves increasingly restrictive sampling from the upper and lower tails of the residual distribution to capture the joint effects of unexpected floods and droughts on the water cycle, while the second involves sampling from the residuals of the millennium drought. These two methods are complemented by applying the RV DCC model to projected climate data from up to 42 global climate models. The empirical results are consistent and predict for reservoirs to have a relatively smaller contribution in the water portfolio, whereas rainwater harvesting and desalination have increasing roles. It is estimated that climate change leads to an annual increase in water supply costs of between 7% and 44% over a 20-year forecast horizon.

The rest of this paper is organized as follows. The statistical effects of climatic conditions on water assets are discussed in Section 2. The RV DCC empirical model of water assets with time varying risks is specified in Section 3. A quasi-maximum likelihood estimator is presented in Section 4, which is applied in Section 5 to estimate the RV DCC water asset model. The empirical results in Section 5 are used to construct an optimal portfolio of water assets in Section 6. Implications of the optimal water portfolio in the presence of climate change are discussed in Section 7, with concluding comments contained in Section 8.

2. The statistical effects of climatic conditions

To motivate the structure of the empirical model of water assets presented in Section 3, the statistical effects of climatic conditions on natural resources is now presented for the case of water. The data consist of monthly reservoir inflows and precipitation for rainwater harvesting for the city of Melbourne from January 1925 to December 2010, which are presented in Figure 1 with descriptive statistics given in Table 1.[6] The descriptive statistics of the two water assets reveal significant differences. The average inflow into reservoirs is 45 mm, with a median inflow of 34 mm and a standard deviation of 36 mm. For rainwater harvesting the mean is 66 mm with a median of 63 mm and a standard deviation of 31 mm. As a result rainwater harvesting has a higher mean and a lower standard deviation than reservoir inflows, reflecting the greater geographical dispersion of rainwater harvesting systems compared to the small number of large scale reservoirs.

[5]The millennium drought represents a period of below average reservoir inflows in Melbourne from 1997 to 2009.

[6]Precipitation is measured using gridded (5 km $\times$ 5 km) monthly data (Raupach, Briggs, Haverd, King, Paget, and Trudinger (2009, 2012)), obtained from the Bureau of Meteorology and averaged according to the geographical overlap with the Melbourne greater city area. Monthly reservoir inflows are obtained by aggregating monthly inflows over the four major reservoirs: Maroondah, O'Shannassy, Thomson, and Upper Yarra, which lie outside Melbourne's greater capital city boundary.

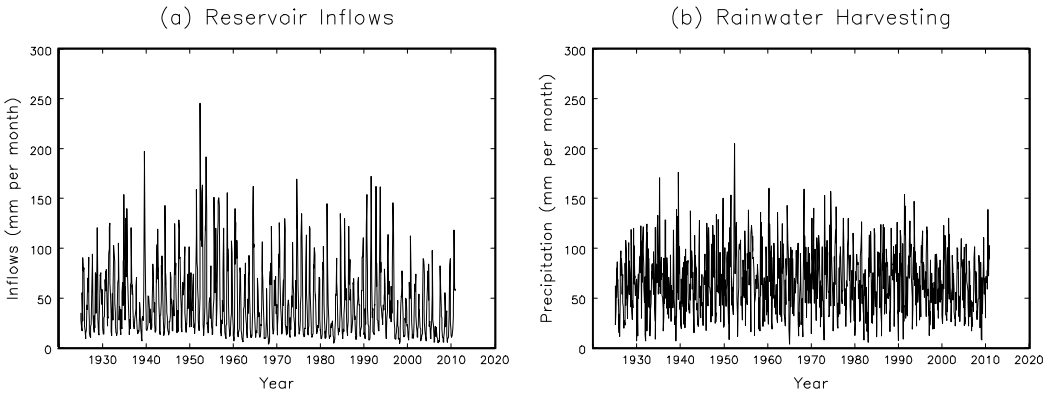

FIGURE 1. Water assets (mm per month), 1925–2010.

The climatic effects on water flows are highlighted in Table 2, which gives the 10 driest and wettest months for reservoir and rainwater harvesting over the sample period. The z-statistic reported represents the number of standard deviations from the mean using the residuals from the seasonal dummy variable regression model. A comparison of the standard deviations reported in the table suggests the driest months are comparatively less extreme than the wettest months. The three driest months for reservoir inflows occur during the Millennium Drought between July and September of 2006, with 2.3 to 2.4 standard deviations below the mean. In contrast, the wettest month is May 1952, representing nearly 8 standard deviations above the mean in the case of reservoir inflows and just under 5 standard deviations above the mean for rainwater harvesting.

Figure 2 provides the empirical distributions of reservoir inflows and rainwater harvesting. The strong positive skewness in reservoir inflows is highlighted in panel (a) where the peak of the distribution occurs between 10 and 15 mm per month. The rainwater harvesting empirical distribution presented in panel (b) exhibits less skewness than reservoir inflows with the peak occurring between 45 and 50 mm per month. By expressing reservoir inflows in logarithms, panel (c) yields an empirical distribution that is more symmetrical. A similar result occurs for the logarithm of rainwater harvesting in panel (d), although the distribution has a thin, left tail.

TABLE 1. Descriptive statistics on water assets (mm per month), 1925–2010.

Statistic	Reservoir Inflows	Rainwater Harvesting
Mean	45.374	66.483
Median	34.025	63.388
Minimum	3.525	3.614
Maximum	245.675	204.942
Standard Deviation	35.962	31.203
Skewness	1.410	0.464
Kurtosis	5.090	3.054

TABLE 2. Extreme events of water assets, 1925–2010. Based on the residuals from a linear regression of the water assets on a set of monthly seasonal dummy variables. The z-statistic reported represents the number of standard deviations from the mean.

Driest Months				Wettest Months			
Reservoirs		Rainwater		Reservoirs		Rainwater	
Date	z-stat	Date	z-stat	Date	z-stat	Date	z-stat
2006, Aug.	−2.424	1934, Apr.	−2.421	1955, Dec.	3.667	1949, Sep.	2.776
2006, Jul.	−2.412	1982, July	−2.268	1952, Oct.	3.903	1970, Feb.	2.926
2006, Sep.	−2.332	1932, Apr.	−2.129	1960, Apr.	4.093	1946, Jan.	2.993
1982, Jul.	−2.288	2006, Sep.	−2.092	1935, Mar.	4.151	1968, Apr.	3.053
1997, Jul.	−2.175	1944, July	−2.075	1944, Apr.	4.209	1960, Apr.	3.099
1982, Aug.	−2.091	2008, Sep.	−1.972	1939, Aug.	4.359	1939, Jul.	3.244
1938, Sep.	−1.993	2005, Apr.	−1.886	1934, Nov.	4.407	1939, Jan.	3.496
2008, Sep.	−1.921	1976, Jun.	−1.862	1953, Sep.	4.535	1935, Mar.	3.807
1967, Jun.	−1.896	1938, Sep.	−1.854	1952, Nov.	4.764	1973, Jan.	4.009
1928, Jul.	−1.890	1967, Sep.	−1.847	1952, May	7.584	1952, May	4.559

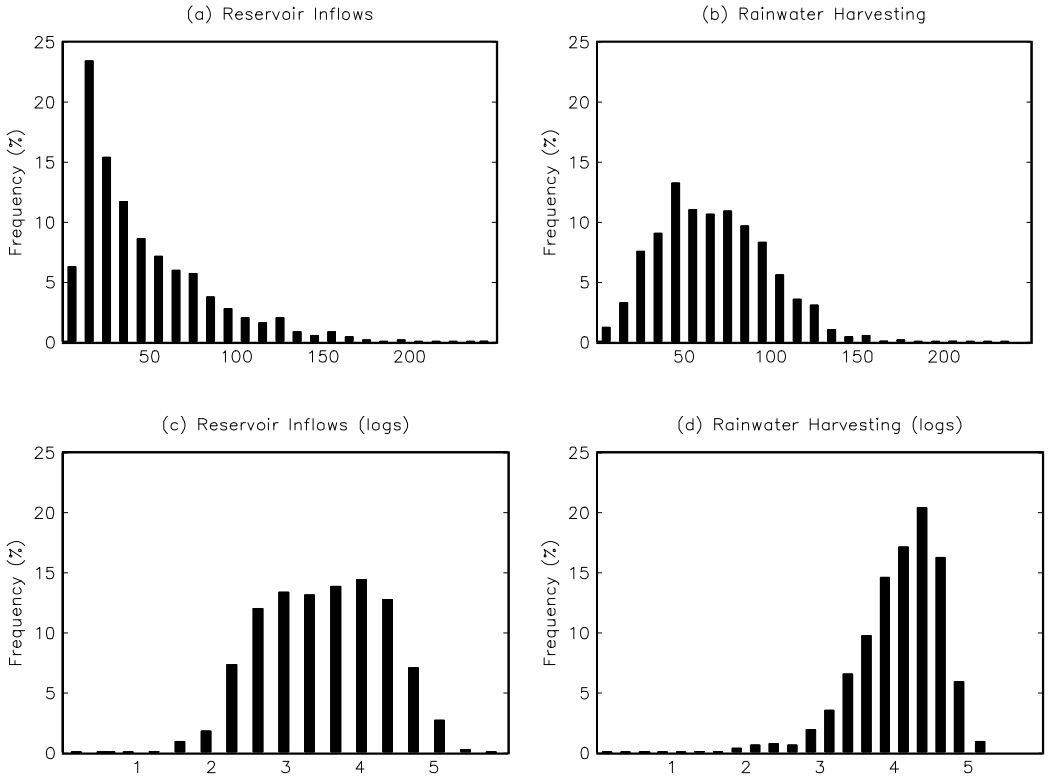

FIGURE 2. Empirical distributions of water assets (*mm* per month), 1925–2010.

TABLE 3. Seasonal factors for reservoir inflows and rainwater harvesting, 1925–2010. Based on a linear regression of the water assets on a set of monthly seasonal dummy variables.

Month	Reservoir Inflows	Rainwater Harvesting
January	0.507	0.651
February	0.352	0.646
March	0.338	0.753
April	0.450	0.995
May	0.696	1.133
June	0.996	1.200
July	1.413	1.277
August	1.861	1.310
September	1.810	1.122
October	1.582	1.116
November	1.168	0.959
December	0.827	0.838

The monthly seasonal patterns for the water assets are given in Table 3. The seasonal factors are the average flows for each month relative to the annual average. A test of no seasonal patterns is rejected for both water assets with p-values of 0.000. A comparison of the seasonal factors for the two water assets shows that reservoir inflows exhibit stronger seasonal variations than rainwater harvesting. Nonetheless, water from from both assets peak in August with water flows being nearly twice the average for reservoirs and just over 30% higher in the case of rainwater harvesting. The lowest inflows for reservoirs occur in March, whereas for harvesting it is one month earlier in February.

Preliminary tests of time varying volatility in the water assets based on the ARCH test of Engle (1982) are given in Table 4. The results of the tests provide strong evidence of time varying volatility in reservoir inflows and rainwater harvesting, with all p-values less than 0.05. To highlight the time variations in the corisks between the two water assets, Figure 3 provides time varying estimates of the correlation using a 12 month rolling window. The dashed line represents the correlation for the total sample period, equal to 0.594. All of the correlations are less than 1.0, providing preliminary evidence that water assets could be combined into a water portfolio to diversify some of the individual asset's risks. Most of the correlations between the two water assets are positive, falling between 0.4 and 0.8. However, there are some periods when the correlations are less than 0.2, and even negative, especially around 1970.

Precipitation data for rainwater harvesting are also available daily from the Bureau of Meteorology for six high quality climate sites: Lovely Banks, Meredith, Portarlington, Toorourrong, Yan Yean, and Wallaby Creek. A monthly realized variance estimate is obtained by integrating the daily variance over each month. Formally, this is achieved by summing the squared daily deviations of each observation from its mean for each month (see Andersen, Bollerslev, Diebold, and Ebens (2001), Barndorff-Nielsen and Shephard (2002), and Aït-Sahalia and Jacod (2014) for a review of realized variance).

TABLE 4. Preliminary tests of time varying volatility in reservoir inflows and rainwater harvesting. Based on tests of ARCH for selected lags 1 to 12 months applied to the residuals from a linear regression of the water assets (in logs) on a constant and a set of seasonal (monthly) dummy variables, with p-values reported in parentheses.

Statistic	Reservoir Inflows	Rainwater Harvesting
ARCH(1)	215.268 (0.000)	11.741 (0.001)
ARCH(2)	231.184 (0.000)	14.345 (0.001)
ARCH(6)	244.245 (0.000)	18.542 (0.005)
ARCH(12)	251.044 (0.000)	24.174 (0.019)

The monthly realized volatility estimates for rainwater harvesting are given in Figure 4 from 1925 to 2010, by taking the square root of the realized variance estimates. The average realized volatility over the period is 20.909 mm, which is less than the corresponding estimate for rainwater harvesting of 31.203 mm reported in Table 1.

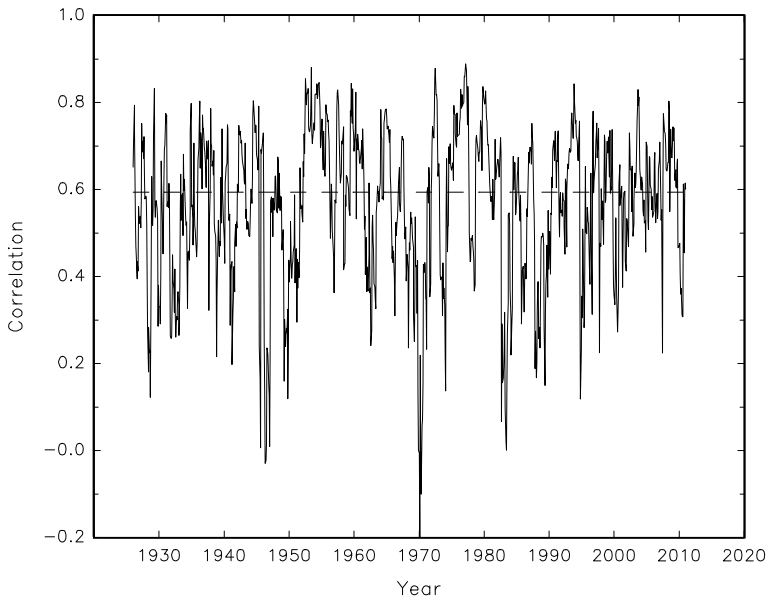

FIGURE 3. Time-varying estimates of the correlation between reservoir and rainwater harvesting assets based on a 12-month rolling window, 1925–2010. The dashed line represents the unconditional correlation for the total sample period, equal to 0.594.

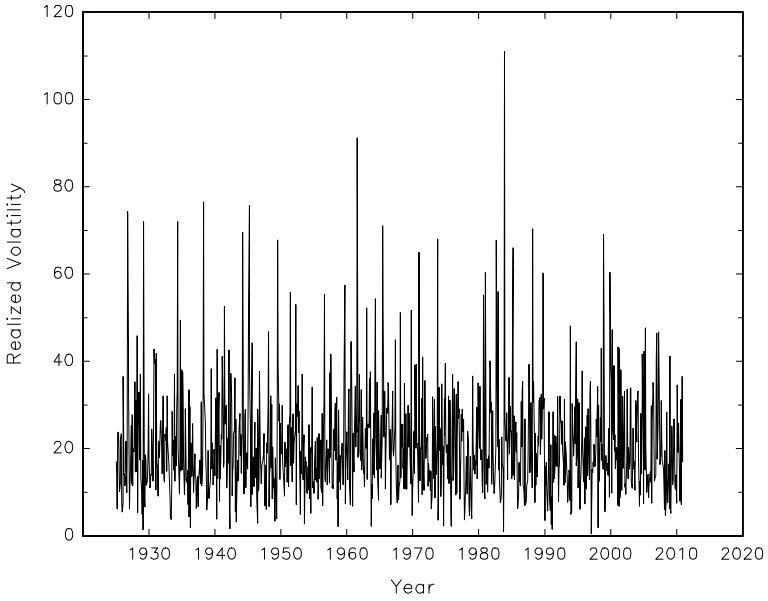

FIGURE 4. Realized volatility of rainwater harvesting (mm per month), 1925–2010.

3. AN EMPIRICAL MODEL OF WATER ASSETS

A bivariate model of water assets with time varying comoments is specified in this section, where the water assets consist of the monthly reservoir inflows and rainwater harvesting given in Figure 1. Time varying variances are modeled using the class of GARCH volatility models of Engle (1982) and Bollerslev (1986). As data on rainwater harvesting are also available daily, the GARCH volatility component of the model for rainwater harvesting is augmented using the realized volatility estimates in Figure 4 based on the RV GARCH model of Hansen, Lunde, and Voev (2012). To capture time variations in the correlations linking the two water assets the Dynamic Conditional Correlation (DCC) model of Engle (2002) is adopted. This class of models is referred to as the RV DCC model.

Let $y_{1,t}$ and $y_{2,t}$ represent respectively logged reservoir inflows and logged rainwater harvesting at time t. The multivariate model of water assets consists of three components. The first component is the model of reservoir inflows specified as

$$\begin{aligned} y_{1,t} &= \phi_{1,0} + \sum_{i=1}^{11} \phi_{1,i} d_{i,t} + u_{1,t}, \\ h_{1,1,t} &= \alpha_{1,0} + \alpha_{1,1} u_{1,t-1}^2 + \beta_{1,1} h_{1,1,t-1}, \\ u_{1,t} &\sim N(0, h_{1,1,t}), \end{aligned} \tag{1}$$

where $d_{i,t}$, $i = 1, 2, \ldots, 11$, are monthly seasonal dummy variables beginning with January, defined as

$$d_{i,t} = \begin{cases} 1: & \text{Month } i, \\ 0: & \text{Otherwise}, \end{cases} \tag{2}$$

in order to capture the seasonal pattern in reservoir inflows, and $h_{1,1,t}$ is the conditional variance of logged reservoir inflows. The disturbance term $u_{1,t}$ captures deviations from expected reservoir inflows corresponding to periods of high inflows ($u_{1,t} > 0$), or dry periods where inflows are below normal levels ($u_{1,t} < 0$). The unexpected movements in reservoir inflows are assumed to have zero mean, with conditional variance $h_{1,1,t}$. Higher volatility in reservoir inflows arises from inflows exhibiting abnormal movements relative to normal levels.

The second component is the rainwater harvesting model, which is specified as

$$\begin{aligned} y_{2,t} &= \phi_{2,0} + \sum_{i=1}^{11} \phi_{2,i} d_{i,t} + u_{2,t}, \\ h_{2,2,t} &= \alpha_{2,0} + \alpha_{2,1} u_{2,t-1}^2 + \beta_{2,1} h_{2,2,t-1} + \beta_{2,2} \log \mathrm{RV}_{t-1}, \\ \log \mathrm{RV}_t &= \delta_0 + \delta_1 h_{2,2,t} + e_t, \\ u_{2,t} &\sim N(0, h_{2,2,t}), \\ e_t &\sim N\big(0, \sigma_e^2\big), \end{aligned} \tag{3}$$

where $d_{i,t}$ are monthly seasonal dummy variables as defined in (2), $h_{2,2,t}$ is the conditional variance of (logged) harvesting, and RV_t is the realized variance of harvesting. The disturbance $u_{2,t}$ captures excess harvesting levels relative to normal levels, which is assumed to have zero mean and conditional volatility $h_{2,2,t}$. The rainwater harvesting conditional variance is represented by a GARCH model augmented by the log of its lagged realized variance. In the empirical finance literature, the realized variance is found to be a good predictor of the latent volatility process, especially during periods where there are large changes in volatilities and correlations (Hansen, Lunde, and Voev (2012)). In the natural resource literature, it is the effects of changing climatic conditions that can result in extreme movements in volatilities and correlations arising from dramatic changes in water flows from periods of floods to periods of droughts. The third expression in (3) represents a measurement equation linking the observed (logged) realized variance $\log \mathrm{RV}_t$, and the unobserved latent variance process of rainwater harvesting $h_{2,2,t}$, with e_t representing the measurement error which is assumed to have zero mean and constant variance σ_e^2 (Hansen, Lunde, and Voev (2012)).[7]

The third component of the model captures time variations in the covariances and correlations between logged reservoir inflows ($y_{1,t}$) and logged rainwater harvesting ($y_{2,t}$). Let H_t represent the conditional covariance matrix between $y_{1,t}$ and $y_{2,t}$ given by

$$H_t = \begin{pmatrix} h_{1,1,t} & h_{1,2,t} \\ h_{1,2,t} & h_{2,2,t} \end{pmatrix}, \tag{4}$$

[7]A number of extensions of the empirical model will be investigated in Section 5, including allowance for seasonality and leverage effects in the conditional variance equations.

where $h_{1,2,t}$ is the conditional covariance between the two water assets. Let the standardized disturbances be defined as

$$z_{1,t} = \frac{u_{1,t}}{\sqrt{h_{1,1,t}}}, \qquad z_{2,t} = \frac{u_{2,t}}{\sqrt{h_{2,2,t}}}, \tag{5}$$

where $u_{1,t}$ is defined in (1) and $u_{2,t}$ defined in (2). The conditional covariance matrix in (4) is expressed as

$$H_t = S_t R_t S_t, \tag{6}$$

with

$$S_t = \begin{pmatrix} \sqrt{h_{1,1,t}} & 0 \\ 0 & \sqrt{h_{2,2,t}} \end{pmatrix}, \qquad R_t = \begin{pmatrix} 1 & \rho_{1,2,t} \\ \rho_{1,2,t} & 1 \end{pmatrix}, \tag{7}$$

where S_t is a diagonal matrix containing the conditional standard deviations of $y_{1,t}$ and $y_{2,t}$, on the main diagonal, and R_t is the correlation matrix with $\rho_{1,2,t}$ representing the time varying conditional correlation between $y_{1,t}$ and $y_{2,t}$. To model the time variation in the conditional correlation, the DCC model of Engle (2002) is adopted by specifying the following pseudo-GARCH covariance matrix

$$Q_t = (1 - \alpha_c - \beta_c)\overline{Q} + \alpha_c z_t z_t' + \beta_c Q_{t-1}, \tag{8}$$

where a_c and β_c are scalar parameters, $z_t = (z_{1,t}, z_{2,t})'$, and

$$\overline{Q} = \frac{1}{T}\sum_{t=1}^{T} z_t z_t', \tag{9}$$

is the unconditional covariance matrix of the standardized disturbances.[8] The time varying correlation is given by

$$\rho_{1,2,t} = \frac{q_{1,2,t}}{\sqrt{q_{1,1,t} q_{2,2,t}}}, \tag{10}$$

where $q_{i,j,t}$ is the i, j element at time t of Q_t.

4. Quasi maximum likelihood estimation

This section provides the details of a quasi maximum likelihood estimator for estimating the parameters of the RV DCC model presented in Section 3. The log-likelihood of the RV DCC model of water assets consists of three components. The first term of the log-likelihood is based on the GARCH conditional volatility model of reservoir inflows. Assuming $u_{1,t}$ in (1) is conditionally normal with zero mean and variance $h_{1,1,t}$, the log-likelihood at observation t is

$$\log L_{1t}(\theta_1) = -\frac{1}{2}\log 2\pi - \frac{1}{2}\log h_{1,1,t} - \frac{1}{2}\frac{u_{1,t}^2}{h_{1,1,t}}, \tag{11}$$

[8] An alternative approach for combining multivariate GARCH models with realized volatility is Hansen, Huang, and Shek (2012). For recent approaches to modeling multivariate realized volatility, see Bollerslev, Meddahi, and Nyawa (2019) and Bollerslev, Patton, and Quaedvlieg (2020).

with unknown parameters

$$\theta_1 = \{\phi_{1,0}, \phi_{1,1}, \ldots, \phi_{1,11}, \alpha_{1,0}, \alpha_{1,1}, \beta_{1,1}\}. \tag{12}$$

The second term of the log-likelihood is based on the RV GARCH conditional volatility model of rainwater harvesting, where $u_{2,t}$ and e_t in (2) are assumed to be independent with conditional normal distributions.[9] The log-likelihood at observation t is (Hansen, Lunde, and Voev (2012))

$$\log L_{2t}(\theta_2) = -\log 2\pi - \frac{1}{2}\log h_{2,2,t} - \frac{1}{2}\log \sigma_e^2 - \frac{1}{2}\frac{u_{2,t}^2}{h_{2,2,t}} - \frac{1}{2}\frac{e_t^2}{\sigma_e^2}, \tag{13}$$

with unknown parameters

$$\theta_2 = \left\{\phi_{2,0}, \phi_{2,1}, \ldots, \phi_{2,11}, \alpha_{2,0}, \alpha_{2,1}, \beta_{2,1}, \beta_{2,2}, \delta_0, \delta_1, \sigma_e^2\right\}. \tag{14}$$

The third term of the log-likelihood corresponds to the time varying correlations between reservoir inflows and rainwater harvesting based on the DCC log-likelihood (Engle (2002))

$$\log L_{3t}(\theta_1, \theta_2, \theta_3) = -\frac{1}{2}\log|R_t| - 0.5 z_t' R_t^{-1} z_t + 0.5 z_t' z_t, \tag{15}$$

where R_t is the correlation matrix in (7) and $z_t = (z_{1,t}, z_{2,t})'$ is the vector containing the standardized disturbances in (5), and the unknown parameters

$$\theta_3 = \{\alpha_c, \beta_c\}. \tag{16}$$

The unknown parameters θ_1 and θ_2 from (12) and (14), respectively, enter the log-likelihood in (15) via the standardized disturbances in z_t.

For a sample of T observations, the full quasi log-likelihood for the RV DCC model is obtained by combining the separate log-likelihoods in (11), (13), and (15), as

$$\begin{aligned}\log L_T(\theta) &= \frac{1}{T}\sum_{t=1}^{T}\big(\log L_{1t}(\theta_1) + \log L_{2t}(\theta_2) + \log L_{3t}(\theta_1, \theta_2, \theta_3)\big) \\ &= \log L_1(\theta_1) + \log L_2(\theta_2) + \log L_3(\theta_1, \theta_2, \theta_3),\end{aligned} \tag{17}$$

where

$$\theta = \{\theta_1, \theta_2, \theta_3\},$$

represents the full set of unknown parameters, and

$$\log L_{1T}(\theta_1) = \frac{1}{T}\sum_{t=1}^{T}\log L_{1t}(\theta_1),$$

[9]The normality assumption for e_t is supported by Andersen et al. (2001), Andersen, Bollerslev, Diebold, and Labys (2003), who provide empirical evidence that realized variance is approximately log-normal.

$$\log L_{2T}(\theta_2) = \frac{1}{T}\sum_{t=1}^{T} \log L_{2t}(\theta_2),$$

$$\log L_{3T}(\theta_1, \theta_2, \theta_3) = \frac{1}{T}\sum_{t=1}^{T} \log L_{3t}(\theta_1, \theta_2, \theta_3).$$

The quasi maximum likelihood estimator is given as the solution of

$$\widehat{\theta}_T = \arg\max_{\theta} \log L_T(\theta), \tag{18}$$

where the asymptotic standard errors are based on the "sandwich" estimator. Under standard regularity conditions, the QMLE is asymptotically distributed as

$$\sqrt{T}(\widehat{\theta}_T - \theta_0) \xrightarrow{d} N(0, \Omega), \tag{19}$$

where θ_0 is the population parameter vector and

$$\Omega = I^{-1}(\theta_0) J(\theta_0) I^{-1}(\theta_0), \tag{20}$$

is the covariance matrix, $I(\theta_0)$ is the information matrix, and $J(\theta_0)$ is the outer product of gradients (OPG) matrix.

The quasi maximum likelihood estimator is computed using the Broyden, Fletcher, Goldfarb, and Shanno iterative gradient algorithm available in the MAXLIK procedure in GAUSS, with all gradients computed numerically. As the log-likelihood in (17) has a recursive structure this property is exploited in computing the maximum likelihood estimates by adopting a three-step estimation procedure to maximize each component of the total log-likelihood separately. This estimation sequence involves maximizing (11) with respect to θ_1 in (12) in the first step. In the second step, (13) is maximized with respect to θ_2 in (14). In the third and final step, (15) is maximized with respect to θ_3 in (16) with z_t replaced by the standardized residuals $\widehat{z}_t = (\widehat{z}_{1,t}, \widehat{z}_{2,t})'$ from the first two stages.

The parameter estimates from the first two steps of the estimation procedure are asymptotically efficient as a result of the block-diagonality structure of the information matrix (Engle (2002)). This is not the case for the parameter estimates of θ_3 in the third step, which are consistent, but not asymptotically efficient as the correct standard errors are a function of all of the parameters in the model. To generate asymptotically efficient parameter estimates of the θ_3 parameters in (16), the following approach is adopted, which extends the approach proposed by Engle (2002).[10] Let the gradient vector for the

[10]An alternative strategy to achieve asymptotic efficiency is to iterate the full log-likelihood model once using the three-step parameter estimates as starting values (Martin, Hurn, and Harris (2013)).

three-step estimator be given by

$$G_T(\theta) = \begin{pmatrix} \dfrac{\partial \log L_1(\theta_1)}{\partial \theta_1} \\ \dfrac{\partial \log L_2(\theta_2)}{\partial \theta_2} \\ \dfrac{\partial \log L_3(\theta_1, \theta_2, \theta_3)}{\partial \theta_3} \end{pmatrix}. \tag{21}$$

The information matrix has the following block diagonal structure:

$$I_T(\theta) = E\begin{pmatrix} \dfrac{\partial^2 \log L_1(\theta_1)}{\partial \theta_1 \partial \theta_1'} & 0 & 0 \\ 0 & \dfrac{\partial^2 \log L_2(\theta_2)}{\partial \theta_2 \partial \theta_2'} & 0 \\ \dfrac{\partial^2 \log L_3(\theta)}{\partial \theta_3 \partial \theta_1'} & \dfrac{\partial^2 \log L_3(\theta)}{\partial \theta_3 \partial \theta_2'} & \dfrac{\partial^2 \log L_3(\theta_3)}{\partial \theta_3 \partial \theta_3'} \end{pmatrix} = \begin{pmatrix} I_a & 0 \\ I_c & I_d \end{pmatrix}, \tag{22}$$

where the partitioned matrices are

$$\begin{aligned} I_a &= E\begin{pmatrix} \dfrac{\partial^2 \log L_1(\theta_1)}{\partial \theta_1 \partial \theta_1'} & 0 \\ 0 & \dfrac{\partial^2 \log L_2(\theta_2)}{\partial \theta_2 \partial \theta_2'} \end{pmatrix}, \\ I_c &= E\begin{pmatrix} \dfrac{\partial^2 \log L_3(\theta)}{\partial \theta_3 \partial \theta_1'} & \dfrac{\partial^2 \log L_3(\theta)}{\partial \theta_3 \partial \theta_2'} \end{pmatrix}, \\ I_d &= E\left(\frac{\partial^2 \log L_3(\theta_3)}{\partial \theta_3 \partial \theta_3'}\right). \end{aligned} \tag{23}$$

From the properties of partitioned inverses,

$$I_T^{-1}(\theta) = \begin{pmatrix} I_a & 0 \\ I_c & I_d \end{pmatrix}^{-1} = \begin{pmatrix} I_a^{-1} & 0 \\ -I_d^{-1}\Psi & I_d^{-1} \end{pmatrix}, \tag{24}$$

where

$$\Psi = I_c I_a^{-1}. \tag{25}$$

Letting $J_T(\theta)$ represent the outer product of gradients matrix associated with (21), the quasi-maximum likelihood covariance matrix is

$$\Omega_T(\theta) = I_T^{-1}(\theta) J_T(\theta) I_T^{-1}(\theta)'. \tag{26}$$

Using (24) in (26) gives

$$\Omega_T(\theta) = \begin{pmatrix} I_a^{-1} & 0 \\ -I_d^{-1}\Psi & I_d^{-1} \end{pmatrix} \begin{pmatrix} J_a & J_b \\ J_c & J_d \end{pmatrix} \begin{pmatrix} I_a^{-1} & -\Psi' I_d^{-1} \\ 0 & I_d^{-1} \end{pmatrix} = \begin{pmatrix} \omega_a & \omega_b \\ \omega_c & \omega_d \end{pmatrix}, \tag{27}$$

where J_a, J_b, J_c, J_d are the conformable elements of the OPG matrix $J_T(\theta)$, and

$$\begin{aligned} \omega_a &= I_a^{-1} J_a I_a^{-1}, \\ \omega_b &= -I_a^{-1} J_a \Psi' I_d^{-1} + I_a^{-1} J_b I_d^{-1}, \\ \omega_c &= \omega_b', \\ \omega_d &= I_d^{-1}\big(J_d - J_c\Psi' - \Psi J_b + \Psi J_a \Psi'\big) I_d^{-1}. \end{aligned}$$

The QMLE covariance matrix of $\widehat{\theta}$ is

$$\operatorname{cov}(\widehat{\theta}_T) = \frac{1}{T}\Omega_T(\widehat{\theta}), \tag{28}$$

with standard errors computed as the square roots of the diagonal elements of this matrix. In evaluating $\Omega_T(\widehat{\theta})$ in the empirical analysis in Section 5, the information matrix is approximated by the Hessian and the OPG matrix $J_T(\theta)$ is evaluated by taking the average of the cross-products of the gradients in (21) over the sample.

5. Empirical results

The quasi-maximum likelihood parameter estimates of the RV DCC time varying risk model of water assets in equations (1) to (10) are given in Table 5 using the monthly data on reservoir inflows and rainwater harvesting in Figure 1, and the realized volatility estimates in Figure 4.[11] As a basis of comparison Table 5 also contains the results of a constant risk benchmark model by restricting the variances and covariances to be time invariant. Comparison of the joint AIC for the two models given in Table 5, computed as $\text{AIC} = -2\log L(\widehat{\theta}) + 2N/T$ where N is the dimension of $\widehat{\theta}$, provides strong support for the time varying risk model. Comparing the AICs for the each of the three subcomponents of the two models further confirms this result with the AIC being minimized for all three submodels of the time-varying risk model.

Inspection of the conditional mean parameter estimates of ϕ_1 to ϕ_{11}, suggests strong evidence of seasonality in the mean of both water assets. Reservoirs have the greatest inflows on average in September (ϕ_9), closely followed by August (ϕ_8) and October (ϕ_{10}). The lowest average inflows occur in February (ϕ_2), followed by March (ϕ_3)

[11] Diagnostic tests for first-order ARCH applied to the standardized residuals show no evidence of misspecification of the conditional volatility. In the case of reservoir inflows the ARCH applied to $\widehat{z}_{1,t}$, yields a p-value of 0.712, whereas for rainwater harvesting the pertinent p-value of the ARCH test is 0.887. A similar qualitative result applies for the covariance of the standardized residuals, which yields a p-value of 0.382.

TABLE 5. Maximum likelihood parameter estimates of the time varying risk model in equations (1) to (10) of reservoir inflows and rainwater harvesting water assets, with QMLE standard errors, 1925–2010. For comparison, the results of estimating a constant risk model are presented by restricting the variances and covariances to being time invariant.

	Time Varying Risk Model				Constant Risk Model			
	Reservoirs		Rainwater		Reservoirs		Rainwater	
Param.	Est.	SE	Est.	SE	Est.	SE	Est.	SE
				Conditional Mean				
ϕ_0	3.557	0.041	3.900	0.064	3.473	0.059	3.896	0.057
ϕ_1	−0.498	0.043	−0.268	0.092	−0.467	0.079	−0.276	0.086
ϕ_2	−0.919	0.054	−0.401	0.099	−0.826	0.080	−0.380	0.098
ϕ_3	−0.915	0.061	−0.158	0.090	−0.851	0.078	−0.136	0.085
ϕ_4	−0.793	0.074	0.118	0.087	−0.649	0.086	0.179	0.079
ϕ_5	−0.324	0.080	0.302	0.080	−0.240	0.089	0.306	0.081
ϕ_6	0.101	0.071	0.428	0.073	0.174	0.085	0.424	0.068
ϕ_7	0.530	0.066	0.499	0.072	0.561	0.082	0.497	0.067
ϕ_8	0.818	0.060	0.510	0.074	0.853	0.079	0.510	0.069
ϕ_9	0.829	0.056	0.389	0.073	0.850	0.075	0.367	0.067
ϕ_{10}	0.654	0.054	0.335	0.080	0.682	0.082	0.318	0.076
ϕ_{11}	0.347	0.050	0.190	0.078	0.354	0.084	0.180	0.072
				Conditional Variance				
α_0	0.088	0.016	0.053	0.045	0.522	0.013	0.489	0.014
α_1	0.484	0.069	0.150	0.059	0.000		0.000	
β_1	0.205	0.089	0.381	0.007	0.000		0.000	
β_2			0.014	0.007	0.000		0.000	
				Realized Variance				
δ_0			5.533	0.183	5.707	0.038		
δ_1			0.724	0.764	0.000			
σ_e			1.233	0.042	1.234	0.042		
				Conditional Covariance				
$\alpha_c \times 10^{-6}$	4.170	1.757			0.000		0.000	
β_c	0.628	0.005			0.000		0.000	
	$\log L_1 = -0.669$		$\text{AIC}_1 = 1.366$		$\log L_1 = -0.770$		$\text{AIC}_1 = 1.565$	
	$\log L_2 = -2.318$		$\text{AIC}_2 = 4.673$		$\log L_2 = -2.333$		$\text{AIC}_2 = 4.696$	
	$\log L_3 = 0.181$		$\text{AIC}_3 = -0.359$		$\log L_3 = 0.156$		$\text{AIC}_3 = -0.311$	
	$\log L = -2.805$		$\text{AIC} = 5.680$		$\log L = -2.947$		$\text{AIC} = 5.950$	

and April (ϕ_4). Rainwater harvesting peaks in August (ϕ_8), while the lowest harvesting occurs in February (ϕ_2) on average.[12]

[12]Extending the reservoir inflows and rainwater harvesting conditional variance equations through the inclusion of seasonal dummy variables reveals weak evidence of seasonality in the water assets volatilities. For reservoir inflows, all of the parameter estimates on the seasonal dummy variables conditional variance are statistically insignificant. In the case of rainwater harvesting, 8 of the 11 parameter estimates on the seasonal dummy variables are statistically insignificant. Moreover, sensitivity analysis from allowing for seasonality in the conditional variance equations presented in footnote 19 suggests no qualitative change in the empirical results.

The parameter estimates of the volatility equations given by α_1, β_1, and β_2, provide strong evidence of time variation in volatility in the two water assets.[13] A comparison of the memory properties of the two volatility processes is given by the half-life of a shock, which is the time it takes for a process to return halfway back to its long-run equilibrium volatility after a shock. The half-life of the reservoir inflows variance is $\log((\alpha_{1,1} + \beta_{1,1})/2)/\log(\alpha_{1,1} + \beta_{1,1})$.[14] The estimate of the half-life is $\log((0.481 + 0.205)/2)/\log(0.481 + 0.205) = 2.839$, or just under 3 months. For rainwater harvesting the half-life is $\log((\alpha_{2,1} + \beta_{2,1} + \beta_{2,2}\delta_1)/2)/\log(\alpha_{2,1} + \beta_{2,1} + \beta_{2,2}\delta_1)$, which takes into account realized volatility.[15] The half-life estimate for rainwater harvesting is $\log((0.150 + 0.381 + 0.014 \times 0.724)/2)/\log(0.150 + 0.381 + 0.014 \times 0.724) = 2.129$, or just over 2 months. These properties of the volatilities of the two water assets are highlighted in Figure 5, which contains estimates of the time varying volatilities of reservoir inflows and rainwater harvesting, as well as the corisk as given by the conditional covariance and correlation.

The parameter estimates for the rainwater harvesting asset also provide strong evidence of the important role of the realized variance in predicting the conditional variance $h_{2,2,t}$, as the parameter estimate of $\beta_{2,2}$ in (3) is statistically significant. The slope parameter estimate of the measurement equation in (3) is $\widehat{\delta_1} = 0.724$, suggesting a positive relationship between $\log \mathrm{RV}_t$ and $h_{2,2,t}$, although this estimate is not statistically significant.

The covariance parameter estimates α_c and β_c of the DCC model in equation (8) are both statistically significant. The estimate of α_c is numerically small suggesting very little random variations in the pseudo covariance Q_t, which combined with the estimate of 0.628 for β_c, yields a half-life between the half-lives obtained for the variances of the two water assets.

Figure 5 contains the time varying risk estimates of reservoir inflows and rainwater harvesting, as well as the corisk as given by the conditional covariance and corre-

[13]Tests for asymmetries in the conditional variance equations for reservoirs and rainwater harvesting are also conducted. The leverage tests for reservoirs are based on specifying the GJR model of Glosten, Jagannathan, and Runkle (1993) and testing for the leverage effect. The empirical results yield a test statistic of 2.167, with a p-value of 0.141, showing that the null of no leverage effect is not rejected. In testing for a leverage effect in the rainwater harvesting conditional variance equation the approach is based on Hansen, Lunde, and Voev (2012), by including powers of the standardized residuals in equation (3). The empirical results yield a test statistic of 0.727, with a p-value of 0.695, showing no evidence of leverage effects in rainwater harvesting.

[14]Engle and Patton (2001) defined the half-life as $|E_t h_{t+k} - h| = 0.5|E_t h_{t+1} - h|$, where h is the long-run variance.

[15]The half-life of the rainwater harvesting variance equation is obtained by using the realized variance equation in (3) to rewrite the conditional variance equation for $h_{2,2,t}$ as

$$h_{2,t} = \alpha_{2,0} + \beta_{2,2}\delta_0 + \alpha_{2,1}u_{2,t-1}^2 + (\beta_{2,1} + \beta_{2,2}\delta_1)h_{2,t-1} + e_{t-1}.$$

For $k \geq 2$, the conditional forecast is

$$E_t(h_{t+k} - h) = (\alpha_{2,1} + \beta_{2,1} + \beta_{2,2}\delta_1)^{k-1}E_t(h_{t+1} - h),$$

which from the Engle and Patton (2001) definition of the half-life and assuming the parameters are positive, is $(\alpha_{2,1} + \beta_{2,1} + \beta_{2,2}\delta_1)^{k-1} = 0.5$. Taking natural logarithms and solving for k gives the expression used in the paper.

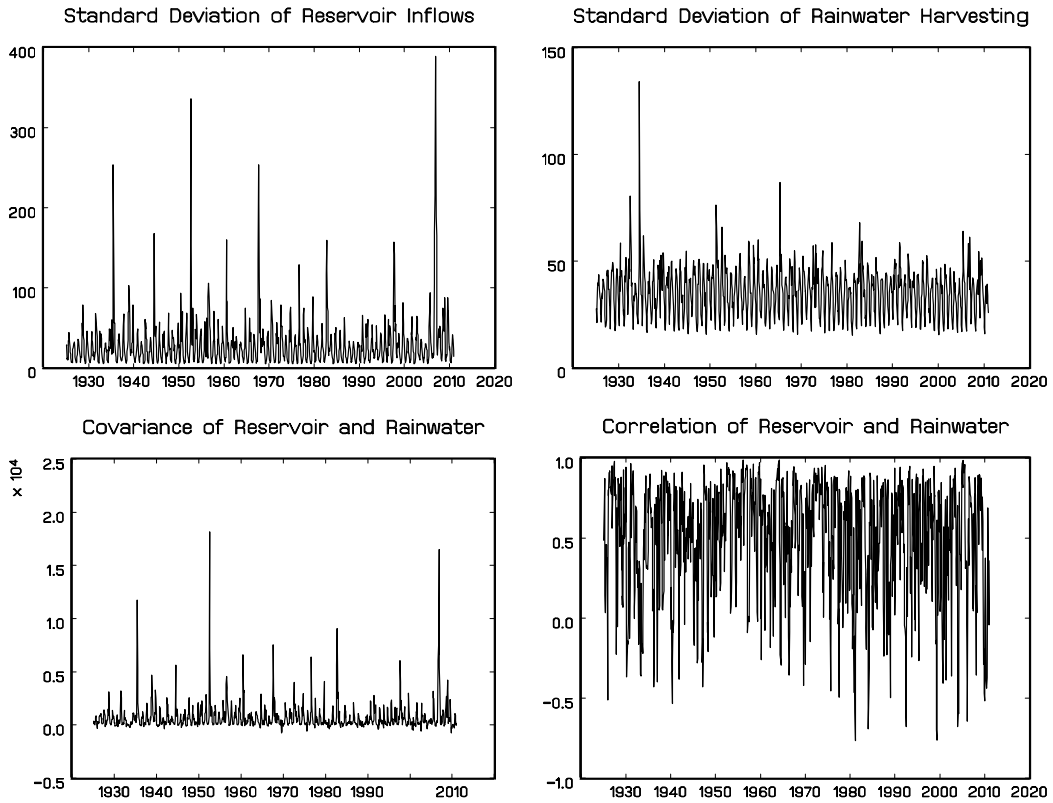

FIGURE 5. Empirical estimates of the time-varying measures of risk between reservoir inflows and rainwater harvesting (in logs), 1925–2010. Based on the estimated bivariate RV-GARCH model in Table 5.

lation, based on the estimated bivariate RV DCC model in Table 5. A comparison of the time varying estimates of the two variances suggests that reservoir inflows exhibit higher volatility than rainwater harvesting. This feature of the empirical results is important as it suggests that even though the capacity of reservoir inflows is much higher than it is for rainwater harvesting, the latter water asset exhibits lower volatility, which can dampen volatility movements of a water portfolio containing both of these water assets.

6. ESTIMATING AN OPTIMAL WATER PORTFOLIO

The empirical results, presented in Section 3, are now used to generate time varying optimal portfolios of water supply. The portfolio consists of the two climate sensitive assets, reservoir inflows, and rainwater harvesting, as well as a third, risk-free asset, desalinated water. The optimal share equations are derived from the water portfolio model of Leroux and Martin (2016) (see Appendix A in the Online Supplementary Material (Leroux, Martin, and St. John (2022)). This is a stochastic dynamic programming model, where a water manager chooses time paths for future water consumption and portfolio allocations from alternative water sources to maximize a discounted intertemporal utility

function subject to a set of constraints representing dynamic equations of water flows from the alternative sources.[16] In this model, reservoir inflows and rainwater harvesting are treated as stochastic water assets. Water from the desalination plant is treated as risk-free in terms of providing reliable supply that is independent of climatic conditions.

The optimal water portfolio share equations for reservoirs, w_1, and rainwater harvesting, w_2, adjusted for costs, are respectively given by

$$w_1 = (k_1 a_1 - k a_2)\gamma^{-1}, \tag{29}$$

$$w_2 = (k_2 a_2 - k a_1)\gamma^{-1}. \tag{30}$$

The cost-adjusted share of desalinated water, w_3, is then determined from the adding up constraint

$$w_3 = 1 - w_1 - w_2 \tag{31}$$

for simplicity the t subscript has been dropped. The parameter γ is the relative risk aversion of the water manager and characterizes the shape of the utility function. In calibrating the model, the risk aversion parameter is assumed to be constant.[17] Water utility managers are risk averse for $\gamma > 0$, with $\gamma > 1$ representing relatively high risk aversion. In the extreme case where $\gamma \to \infty$, the optimal solution is not to source any water from the two risky water assets ($w_1 = w_2 = 0$), but only from desalinated water ($w_3 = 1$).

The terms

$$a_1 = \frac{\mu_1}{S_1} - \frac{\mu_3}{S_3} + \frac{c_1\lambda_1}{p}\left(\mu_1 + \frac{\sigma_1^2}{S_1}\right) - \frac{c_3\lambda_3\mu_3}{p}, \tag{32}$$

$$a_2 = \frac{\mu_2}{S_2} - \frac{\mu_3}{S_3} + \frac{c_2\lambda_2}{p}\left(\mu_2 + \frac{\sigma_2^2}{S_2}\right) - \frac{c_3\lambda_3\mu_3}{p}, \tag{33}$$

in (29) and (30) represent respectively the cost-adjusted excess water flows from reservoirs and rainwater harvesting relative to desalinated water, and S_i is asset $i's$ water stock. The parameters μ_i and σ_i are respectively the mean and standard deviation of asset $i's$ water flows, $c_i = (K_i + O_i(S_i))/S_i$ is the average cost per unit of water, where K_i are capital costs and O_i are operating costs. Finally, the price of water is p and $\lambda_i = p(K_i + O_i - O_i' S_i)/(K_i + O_i)^2$, where $O_i' = dO_i/dS_i$ and the remaining terms k_1, k_2, and k, are the risk-adjusted terms defined as

$$k_1 = \frac{1}{\left(1 - \rho_{12}^2\right)\left(\frac{\sigma_1}{S_1} + \frac{\sigma_1 c_1 \lambda_1}{p}\right)^2},$$

$$k_2 = \frac{1}{\left(1 - \rho_{12}^2\right)\left(\frac{\sigma_2}{S_2} + \frac{\sigma_2 c_2 \lambda_2}{p}\right)^2}, \tag{34}$$

[16]The Leroux–Martin (2016) model is based on a stochastic dynamic optimization framework, which is in contrast to the static portfolio model proposed by Humphreys and McClain (1998).

[17]See Leroux, Martin, and Zheng (2018) for an alternative utility function in a water portfolio model where the relative risk aversion parameter is allowed to be time-varying.

$$k = \rho_{12}\sqrt{k_1 k_2},$$

where ρ_{12} is the correlation between reservoir inflows and rainwater harvesting.

Before constructing the optimal water portfolio shares it is necessary to convert the conditional mean and the conditional variance and co-volatility estimates obtained in Section 3, into the appropriate quantities used in equations (29) and (30). This also captures the relative size and performance of the water assets, described in detail in Leroux and Martin (2016). The empirical estimates of the conditional moments of reservoir inflows are measured in mm. To convert these estimates into a volumetric measure of reservoir inflows, conditional means and variances are scaled by the total catchment area of reservoirs, estimated at 1071.5 km^2 and annualized by scaling these conditional moments by 12. In the case of harvested rain, the catchment area of a representative harvesting site is 3.6 km^2. Assuming a harvesting rate of 0.1 the rainwater harvesting conditional moments are scaled by 0.36 km^2 and annualized while taking into account the capacity constraints of harvesting technology. Finally, the average flow of desalinated water from the desalination plant given by μ_3 is chosen based on the scenario investigated in the calibration experiments.[18]

The parameter values used to calibrate the water portfolio are summarized in Table 6. Reservoirs have the greatest storage capacity of $S_1 = 1290$ GL. The storage capacity for a rainwater harvesting site is $S_2 = 0.217$ GL while the maximum capacity for the desalination plant is $S_3 = 150$ GL, which is designed to provide one-third of Melbourne's water supply during drought conditions. Reservoirs also incur the highest capital costs, with desalination costs being roughly half that of reservoirs, while harvesting has the lowest. In contrast, reservoirs have the lowest operating costs with desalination having the highest.

The price of water is set at $p = 2.47$\$/kL, which is taken as the wholesale price of water in 2013/14 (Melbourne Water (2013)). The population growth for the city of Melbourne is set at $\xi = 2\%$ per annum (ABS (2015)). The discount rate is $\delta = 3\%$ per annum, which is chosen to reflect the long term planning horizon of urban water infrastructure projects and the risk aversion parameter γ, is set at 3.5, based on the empirical analysis in Leroux and Martin (2016).

The conditional means and comoments from the estimated model in Section 5 are expressed in terms of the logarithms of the water assets. Given the assumption of normality used in specifying (1) to (3), the conditional means of the levels of the water assets are

$$\begin{aligned} \mu_{1,t} &= \exp(m_{1,t} + 0.5h_{1,1,t}), \\ \mu_{2,t} &= \exp(m_{2,t} + 0.5h_{2,2,t}), \end{aligned} \tag{35}$$

[18]The modeling incorporates technological change in the water sector by explicitly modeling new technologies such as desalination and rainwater harvesting. Reservoirs have been operating essentially unchanged since the beginning of the last century. In contrast, potential efficiency gains in rainwater harvesting can be accommodated in this model via changes in the harvesting rate. For details, see Leroux and Martin (2016).

TABLE 6. Calibration parameter values used to calibrate the portfolio water model, equations (29) to (34) for Melbourne.

Parameter	Value	Unit	Description
S_1	1290	GL	Reservoir capacity
S_2	0.217	GL	Rainwater capacity
S_3	150	GL	Desalination plant capacity
K_1	1166	\$$m$	Reservoir fixed capital costs, p.a.
K_2	0.39	\$$m$	Rainwater fixed capital costs, p.a.
K_3	656	\$$m$	Desalination fixed capital costs, p.a.
o_1	0.00	\$/kL	Reservoir operating costs per unit
o_2	0.29	\$/kL	Rainwater operating costs per unit
o_3	1.08	\$/kL	Desalination operating costs per unit
p	2.47	\$/kL	Water price
ξ	0.02		Population growth rate, p.a.
δ	0.03		Discount rate, p.a.
γ	3.50		Risk aversion parameter

where

$$\begin{aligned} m_{1,t} &= \phi_{1,0} + \sum_{i=1}^{11} \phi_{1,i} d_{i,t}, \\ m_{2,t} &= \phi_{2,0} + \sum_{i=1}^{11} \phi_{2,i} d_{it}, \end{aligned} \tag{36}$$

are the conditional means of the two water assets. The corresponding conditional variances are

$$\begin{aligned} \sigma_{1,t}^2 &= \exp(2m_{1,t} + h_{1,1,t})\big(\exp(h_{1,1,t}) - 1\big), \\ \sigma_{2,t}^2 &= \exp(2m_{2,t} + h_{2,2,t})\big(\exp(h_{2,2,t}) - 1\big), \end{aligned} \tag{37}$$

while the conditional covariance is

$$\sigma_{1,2,t} = \exp\big(m_{1,t} + m_{2,t} + 0.5(h_{1,1,t} + h_{2,2,t})\big)\big(\exp(h_{1,2,t}) - 1\big). \tag{38}$$

The conditional correlation of the levels of reservoir inflows and rainwater harvesting is defined as $\sigma_{1,2,t}/(\sigma_{1,t}\sigma_{2,t})$. Evaluating the conditional moments in (35) to (38) based on the quasi maximum likelihood estimates in Section 5, yields the estimates of the conditional second-order moments used in the calculation of the optimal water portfolio. The optimal portfolio weights in equations (29)–(31) are evaluated by substituting the estimated conditional variances and covariance in equations (32)–(34).

In constructing the optimal water supply portfolio, the system is assumed to be operating in normal times with water stocks based on their long run historical values. In the case of reservoirs, the mean capacity utilization over the past 25 years is approximately 65% (Melbourne Water (2018)). This implies an effective stock of $S_1 = 1290 \times 0.65 =$

838.5, with average per unit costs of

$$c_1 = \frac{K_1}{S_1} + o_1 = \frac{1166}{1290 \times 0.65} + 0.00 = 1.3906.$$

The long run average for rainwater harvesting is set at 75%, which is taken from Leroux and Martin (2016). The effective stock of harvested water is then $S_2 = 0.217 \times 0.75 = 0.1627$, with average per unit costs of

$$c_2 = \frac{K_2}{S_2} + o_2 = \frac{0.39}{0.217 \times 0.75} + 0.29 = 2.6863.$$

Average unit costs of desalinated water are computed as if the desalination plant is operating at full capacity, given by

$$c_3 = \frac{K_3}{S_3} + o_3 = \frac{656}{150} + 1.08 = 5.4533.$$

It is assumed that the average flow of desalinated water is 40% of capacity.

The results of the calibration for the base case are presented in columns 2 to 4 of Table 7. The average contributions of the water assets suggests that reservoirs contribute 87% of the total cost-adjusted water stock, with the remaining water coming from rainwater harvesting (8%) and desalination (5%). The median for reservoir inflows is slightly higher at 95%, reflecting the presence of past positive outliers in reservoir inflows. The standard deviations indicate some variation in the optimal portfolio over time, especially in the case of desalination, which has a standard deviation of 14%. The total cost of the water portfolio is estimated to be $1.67 bn per year for the base case, which is calculated from the asset shares, the average unit supply costs from each water asset and the total cost-adjusted water stock. The long run average portfolio composition and costs resulting from the base case are in line with the results for long run average conditions under assumptions of constant risks and corisks, presented in columns 5 to 7 of Table 7. However, as suggested by the low frequency with which desalination is used, and as seen in the subsequent analyses, long run averages mask important variations in asset shares from one year to the next as well as marked differences in the frequency of use of alternative water assets that can only be unveiled if one allows for time varying risk.[19]

Figure 6 plots the optimal cost-adjusted portfolio shares from reservoirs and rainwater harvesting for the full sample period alongside each water asset's conditional variance and the conditional correlation. The top panel suggests that reservoirs tend

[19]Some sensitivity experiments of the estimated model were conducted. Reestimating the time-varying risk model by including seasonal dummy variables in the conditional variance equations does not change the qualitative results presented in Table 7. The average estimates of the weights decrease marginally from 0.87 to 0.85 for reservoir inflows, increase marginally from 0.08 to 0.10 for rainwater harvesting, and remain unchanged at 0.05 for desalination. The percentage number of years in using desalinated water remains at 12.79%, while the cost of the water portfolio increases marginally from $1.67 bn p.a. to $1.70 bn. A second sensitivity experiment consisted of investigating the effects of changes in costs on the portfolio composition. The results suggest variations in the cost structure have minor effects on the water portfolio, with the main effects dominated by the conditional second-order moments and comoments.

TABLE 7. Summary measures of water portfolio weights, 1925–2010, for the base case scenario optimal portfolio composition (p.a.). Columns 2–4 report the average time varying shares computed from optimal monthly water portfolios based on equations (29) to (34) evaluated using the parameter values as per Table 6 and the parameter estimates of the RV DCC model reported in columns 2–5 in Table 5. Columns 5–7 report the optimal portfolio based on the constant risk estimates reported in columns 6–9 in Table 5. *Desal Use* refers to the percentage of years in which desalination optimally contributes to the total cost-adjusted water stock. *Costs* report the average annual total supply cost of the optimal water portfolios.

	Asset Shares[a]					
	Time Varying Risk			Constant Risk		
Statistics	Reservoir	Rainwater	Desal.	Reservoir	Rainwater	Desal.
Average	0.87	0.08	0.05	0.93	0.07	0.00
Median	0.95	0.05	0.00	0.93	0.07	0.00
SD	0.20	0.07	0.14	0.00	0.00	0.00
Desal. Use (% of yrs)			12.79			0.00
Costs ($bn p.a.)			1.67			1.46

[a]Based on a desalination flow of $\mu_3 = 0.4$, stocks of $S_1 = 0.65$ and $S_2 = 0.75$, which represent the average stocks over the last 25 years of our data. A nonnegativity restriction is imposed on some shares.

to dominate the water supply, with reservoirs contributing more than 90% to the water stock over most of this period. Exceptional falls in reservoir shares coincide with increases in the conditional variance of reservoir inflows, giving rise to greater hedging opportunities among alternative water assets. These movements are captured in the theoretical model, for example, in 2006, when decreases in reservoir inflows by nearly 60% are reflected in large increases in reservoir volatility resulting in an exceptionally small portfolio weight allocated to reservoirs and correspondingly larger shares for rainwater harvesting and desalination. The year 2006 was also a record year for water stocks with reservoir levels falling to 30% of capacity, motivating the decision to build Melbourne's desalination plant. The bottom panel suggests that the extent to which rainwater harvesting is used to hedge against greater reservoir risk depends on the conditional variance of rainwater harvesting as well the conditional correlation coefficient between reservoir inflows and rainfall, plotted in the middle panel.

Table 8 reports the optimal water portfolios for the last 20 years of the data, between 1991 and 2010. Reservoirs remain the dominant supply, with rainwater harvesting adding between 2% and 25% to the total cost-adjusted water stock since 1991. Desalinated water does not commonly feature in the optimal water portfolio, except during the years 1997, 2006, and 2007, when desalinated water contributes between 1/4 to almost 2/3 of the total cost-adjusted water stock. These years also coincide with the highest rainwater harvesting contributions over this period. These exceptional years fall within the Millennium Drought, a period of below average reservoir inflows starting in 1997 and ending in 2009. While the desalination plant, commissioned in 2006 and completed in 2012, was built to provide water security in periods of severe water stress such as during the Millennium Drought, these results suggest that the desalination plant would have

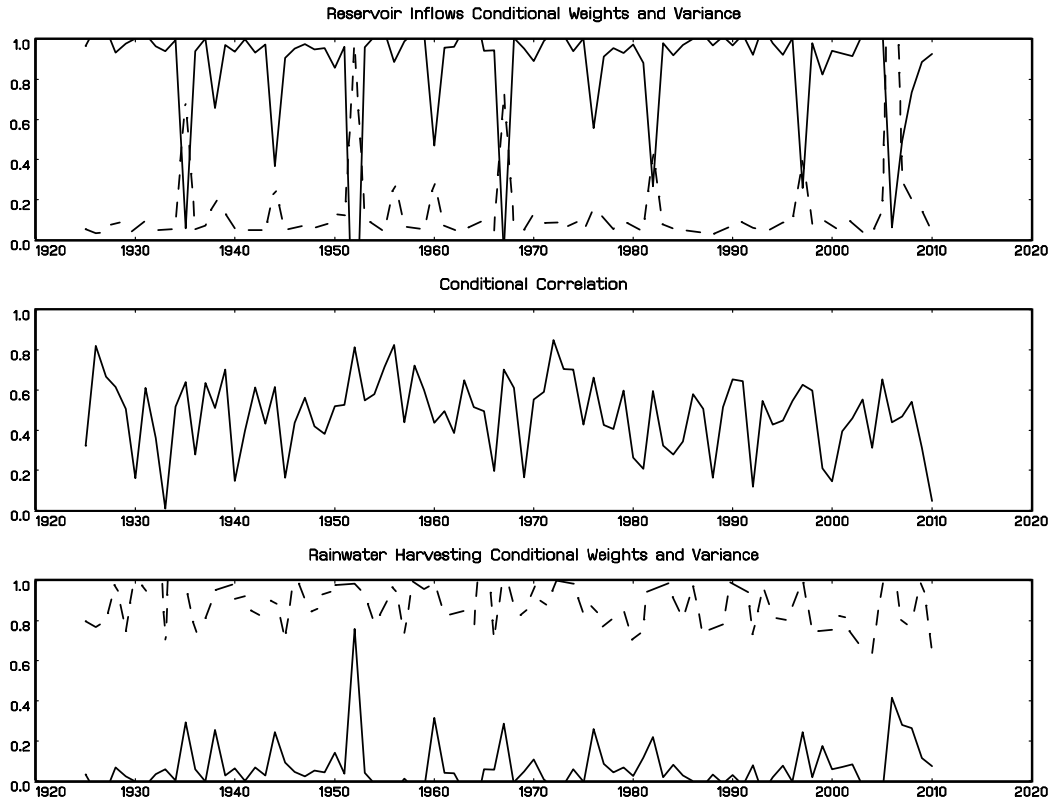

FIGURE 6. Time-varying optimal portfolio shares for reservoir inflows and rainwater harvesting water assets (continuous line), with their conditional variances (long dashed line) and conditional correlations (short dashed line), 1925–2010. The cost-adjusted portfolio share are based on equations (29) to (34), evaluated using the parameter values in Table 6 and the parameter estimates of the RV-GARCH model reported in Table 5.

optimally supplied water in only 3 of the 12 drought years—albeit significant quantities on each occasion.[20]

Before 1997, the operating costs of the optimal water portfolio are mostly stable between \$1.41 bn and \$1.48 bn per year. After this time, the costs vary significantly, with operating costs about twice the long run average operating cost during desalination years.

7. IMPLICATIONS OF CLIMATE CHANGE

The portfolio model in Section 6 is now used to estimate the effects of climate change on the future water portfolio. Two distinct approaches are contrasted. The first approach is

[20]It would be of interest to compare the composition of the conditional water portfolio with the ex-post optimal portfolio composition. However, as the second-order moments are not observed and the third asset did not exist over the sample period, this is not possible. An alternative strategy is to follow the counterfactual experiment in Leroux and Martin (2016).

TABLE 8. Estimated optimal portfolio compositions and costs, 1991–2010. Reported are annual shares computed from optimal monthly water portfolios based on equations (29) to (34), evaluated using the parameter values in Table 6 and the parameter estimates of the RV DCC model reported in columns 2–5 of Table 5. *Costs* give the annual total supply costs of the optimal water portfolios.

	Asset Shares[b]			Costs
Year[a]	Reservoir	Rainwater	Desalinated	($bn p.a.)
1991	0.94	0.06	0.00	1.45
1992	0.95	0.05	0.00	1.44
1993	0.98	0.02	0.00	1.41
1994	0.97	0.03	0.00	1.41
1995	0.91	0.09	0.00	1.48
1996	0.92	0.08	0.00	1.48
1997	0.40	0.22	0.38	3.17
1998	0.94	0.06	0.00	1.45
1999	0.88	0.12	0.00	1.53
2000	0.98	0.02	0.00	1.41
2001	0.94	0.06	0.00	1.46
2002	0.89	0.11	0.00	1.51
2003	0.98	0.02	0.00	1.40
2004	0.99	0.01	0.00	1.39
2005	0.85	0.15	0.00	1.57
2006	0.12	0.25	0.63	4.25
2007	0.51	0.25	0.24	2.65
2008	0.80	0.20	0.00	1.64
2009	0.86	0.14	0.00	1.55
2010	0.97	0.03	0.00	1.41

[a]The years 1997 to 2009 coincide with the Millennium Drought.

[b]Based on a desalination flow of $\mu_3 = 0.4$, stocks of $S_1 = 0.65$, and $S_2 = 0.75$, which represent the average stocks over the last 25 years of our data. A nonnegativity restriction is imposed on some shares.

based on simulating the RV DCC model over a 20-year forecast horizon using a bootstrap resampling scheme applied to the residuals of the model.[21] In the second approach, the RV DCC model estimates are applied to projected climate data, generated from global climate models for four different climate change scenarios over the same 20-year time horizon, ending in 2030. The first approach is internally consistent as it preserves time variations in the variances and covariances of the climate data at the local scale. In contrast, the second approach is based on deterministic approximations of the highly complex physical and biochemical processes and interactions in the global climate system, whereby uncertain initial conditions and future emission pathways result in increasingly uncertain future climates as one moves from a global to a local scale.

[21]The choice of a 20-year forecast horizon is motivated by the remaining life of the desalination plant.

7.1 *Simulating climate change from historical data*

In simulating the RV DCC model, two alternative resampling schemes are investigated. The first scheme involves sampling from both tails of the distribution of the RV DCC residuals to capture the increased frequencies of droughts and floods as projected under climate change (Stocker et al. (2014)). The second scheme replicates extreme events in the recent past by only sampling from the distribution of residuals during a period referred to as the Millennium Drought (1997–2009).[22] For both schemes, the number of bootstrap runs is set at 100,000. For all bootstrap draws, the samples are paired to preserve the correlation structure between reservoir inflows and rainwater harvesting.[23] Sampling from the distribution of estimated values of the RV DCC model parameters as reported in columns 2 to 5 in Table 5 allows explicitly for model uncertainty, whereby less precisely estimated parameter values result in more variable water portfolios across the set of bootstrap draws. For the parameters that are related to the water portfolio model, long term average values as reported in Table 6 are used.

Table 9 reports the results of the first bootstrapping scheme where sampling is obtained from the combined lower and upper tails of the distribution of residuals for various cutoffs. The results reported for various scenarios are the average shares of each water asset over the 20-year horizon, the proportion of years where the desalination plant is used and the cost of the water portfolio. For comparative purposes, the first scenario of the table reports the results from sampling from the full distribution (labeled "All"). The next scenario is from the lower and upper 0.48 tails of the distribution, while the most extreme scenario presented involves sampling from the lower and upper 0.35 tails of the distribution. The results of the simulation experiment demonstrate that by progressively sampling more and more from the lower and upper tails of the distribution the contributions from reservoirs in the water portfolio decrease, while increasing for rainwater harvesting and desalinated water. For the most extreme case where sampling is from the lower and upper 0.35 tails, the contribution from reservoirs decreases from 87% to 66%, whereas for rainwater harvesting the share increases from 8% to 12% relative to the base case in Table 7. The effect on desalination is even more significant with the share allocated to desalination increasing more than fourfold from 5% to 22%, and the proportion of years where desalination is used increasing from one in five years to almost every other year. A comparison of the costs of the water portfolios suggests that water costs increase from \$1.67 bn to \$2.40 bn, an increase of 44% as a result of the most extreme climate change simulation presented in Table 9.

Table 10 reports the results from the second bootstrapping scheme where sampling occurs only from the residuals of the Millennium Drought. This approach adopts capacity utilizations of 50% and 60%, respectively, for reservoirs and harvested rainwater, reflecting the average utilization during the Millennium Drought. The average per unit

[22] A process of whitening and recoloring of the residuals is applied so as to preserve the original autocorrelation in both resampling schemes.

[23] In empirical finance, the proposed methodology of this paper is also used by Brownlees and Engle (2016) to compute the expected marginal shortfall for a given forecast horizon by bootstrapping a multivariate GARCH model.

TABLE 9. Simulated water portfolio results based on a 20-year forecast horizon where sampling is from the combined lower and upper tails of the residual distribution with the cutoff points given in the first column. The number of bootstraps is 100,000. Reported are the average annual shares computed from optimal monthly water portfolios based on equations (29) to (34) evaluated using the parameter values as per Table 6 and the RV DCC parameter estimates drawn from their estimated distributions reported in columns 2–5 of Table 5. *Desal Use* refers to the percentage of years in which desalination optimally contributes to the total cost-adjusted water stock. *Costs* report the average annual total supply cost of the optimal water portfolios.

		Asset Shares[a]		
Sampling	Statistics	Reservoir	Rainwater	Desal.
	Mean	0.87	0.07	0.06
	Median	0.96	0.04	0.00
All	SD	0.23	0.07	0.17
	Desal. Use (% of yrs)			14.32
	Costs ($bn p.a.)			1.71
	Mean	0.85	0.07	0.08
	Median	0.96	0.04	0.00
0.48	SD	0.25	0.07	0.19
	Desal. Use (% of yrs)			17.24
	Costs ($bn p.a.)			1.77
	Mean	0.82	0.08	0.10
	Median	0.95	0.05	0.00
0.45	SD	0.28	0.08	0.22
	Desal. Use (% of years)			21.28
	Costs ($bn p.a.)			1.86
	Mean	0.76	0.10	0.14
	Median	0.93	0.07	0.00
0.40	SD	0.32	0.08	0.25
	Desal. Use (% of yrs)			30.56
	Costs ($bn p.a.)			2.08
	Mean	0.66	0.12	0.22
	Median	0.89	0.11	0.00
0.35	SD	0.36	0.09	0.29
	Desal. Use (% of yrs)			43.91
	Costs ($bn p.a.)			2.40

[a]Based on a desalination flow of $\mu_3 = 0.4$, stocks of $S_1 = 0.65 \times 1290$, and $S_2 = 0.75 \times 0.217$, which represent the average stocks over the last 25 years of the data. A nonnegativity restriction is imposed on some shares.

costs of the two water assets are respectively,

$$c_1 = \frac{K_1}{S_1} + O_1 = \frac{1166}{1290 \times 0.5} + 0.00 = 1.8078,$$

and

$$c_2 = \frac{K_2}{S_2} + O_2 = \frac{0.39}{0.217 \times 0.6} + 0.29 = 3.2854.$$

TABLE 10. Simulated water portfolio results based on a 20-year forecast horizon where sampling is from the residuals of the Millennium Drought. The number of bootstraps is 100,000. Reported are the average annual shares computed from optimal monthly water portfolios based on equations (29) to (34) evaluated using the parameter values as per Table 6 and the RV DCC parameter estimates drawn from their estimated distributions reported in columns 2–5 of Table 5. *Desal Use* refers to the percentage of years in which desalination optimally contributes to the total cost-adjusted water stock. *Costs* report the average annual total supply cost of the optimal water portfolios.

	Asset Shares[a]		
Statistics	Reservoir	Rainwater	Desalinated
Mean	0.77	0.09	0.14
Median	0.93	0.07	0.00
SD	0.30	0.07	0.24
Desal. Use (% of yrs)			30.74
Costs ($bn p.a.)			1.93

[a]Based on a desalination flow of $\mu_3 = 0.5$, and stocks of $S_1 = 0.50 \times 1290$, and $S_2 = 0.60 \times 0.217$, which represent the average stocks during the Millennium Drought. A nonnegativity restriction is imposed on some shares.

In the case of desalinated water, the same average costs apply as for the base case scenario as it is assumed that the desalination plant is operating at constant per unit costs of $c_3 = 5.4533$, for an average annual flow of desalinated water of $\mu_3 = 0.5 = 75$ GL.

Simulating Millennium Drought conditions over the next 20 years, Table 10 suggests an average optimal water portfolio consisting of 77% from reservoirs, while rainwater harvesting and desalination contribute 9% and 14%, respectively, to the total cost-adjusted water stock. Over the 20-year period desalinated water is used more than 30% of the time. The total cost of the water portfolio is $1.93 bn per annum, suggesting a 16% increase in water costs when compared with the baseline cost of $1.67 bn in Table 7.

Tables 9 and 10 are replicated as Tables S1 and S2 in Appendix B in the Online Supplementary Material using the point estimates of the RV DCC parameters as reported in columns 2 and 4 in Table 5. Comparing the computed portfolios and standard deviations of Tables 9 and 10 with those in Appendix B reveals only minor differences, suggesting that the uncertainty in future water portfolios is primarily driven by climate uncertainty with model uncertainty contributing a relatively small amount to overall uncertainty.

7.2 *Water portfolios under projected climate change*

An alternative to generating 20-year forecasts from historical data as a means to simulate climate change is to apply the RV DCC model to projected climate data generated from global climate models for various future warming scenarios.[24] In particular, the

[24]We thank an anonymous reviewer for suggesting that we apply the RV-DCC model also to projected climate data.

projected rainwater harvesting and temperature from up to 42 global climate models for four representative concentration pathway (RCP) scenarios until 2030 is used to generate local projections for rainwater harvesting and reservoir inflows and to compute the optimal future water portfolios under projected climate change.[25] The global climate models and their outputs used here underpin the IPCC's fifth Assessment Report, whereby RCP2.6, RCP4.5, RCP6.0, and RCP8.5 represent respectively higher cumulative future emissions and correspondingly more severe climate change by 2100 (Stocker et al. (2014)).

The 42 climate models differ in their comprehensiveness and the detail and scale with which the complex physical and biochemical processes and feedbacks in the climate system are modeled and so provide a good basis for understanding the role of uncertainty between models in projecting future water portfolios. Yet, common to all models is their deterministic nature, whereby within model uncertainty is generated from different initial conditions rather than from the stochastic approach adopted in Section 7.1. This has interesting implications for interpreting optimal future water portfolios that arise when applying the RV DCC model, which explicitly allows for time varying covariance matrices, to projected climate data.

Columns 3–5 in Table 11 present the portfolios that arise under the four different climate change projection scenarios and the assumption of time varying risks and co-risks. It is immediately apparent that the four climate change scenarios do not result in consistently larger shares of harvested and desalinated water as is seen in Table 9. Instead the results demonstrate pairwise consistency with reservoir shares decreasing between RCP2.6 and RCP6.0 as well as between RCP4.5 and RCP8.5, but not, for example, between RCP2.6 and RCP4.5. This result is potentially due to the different assumptions regarding the timing and height of global emission peaks across the RCP scenarios, whereby some low emission scenarios feature highly concave emission pathways with increases in emissions in the earlier decades followed by rapidly decreasing emissions in the latter half of this century.

Overall, the rebalancing of the water portfolio toward more desalinated water that is observed between RCP2.6 and RCP6.0 mimics more closely the forecasting results that are obtained from simulating the RV DCC model in Section 7.1. The share of desalinated water increases from 4% to 9% and the frequency of its use doubles from around one in 6 years to 1 in 3 years. This has consequences for the projected water portfolio costs, which increase, relative to the long run average historical costs, by 32% to $2.21 bn for RCP6.0.

[25]Projected precipitation and temperature data was downloaded for Melbourne and the catchment areas. To generate projected reservoir inflows under the RCP scenarios, a precipitation-runoff model (PERM) was used as described in Peel, Srikanthan, McMahon, and Karoly (2015). The model runs on a monthly time step with 5 parameters to be optimized and was calibrated to observed (BOM AWAP) rainfall, temperature, and reservoir inflow data. The downloaded precipitation and temperature projections were stochastically replicated 100 times, quantile-quantile bias corrected using historical precipitation and temperature data and run through the calibrated PERM model giving runoff projections. To generate projected harvested rainwater, grid cell coordinates, and cell weights were used to determine weighted average precipitation projections for the Melbourne Greater Capital City Area. The weighted average precipitation projections were stochastically replicated 100 times and then quantile-quantile bias corrected using historical precipitation data.

Across all climate change scenarios the shares of rainwater harvesting are higher, ranging from 22% to 37%, than under RV DCC climate change forecasts.

Assuming constant risk in projected climate data results in much less variation in projected water portfolios across the four climate change scenarios as demonstrated in columns 6 to 8 in Table 11. With around 93% of water being sourced from reservoirs and the remainder being rainwater harvesting, there is no significant case for desalination even under the most severe climate change scenarios. As a result, projected water portfolio costs under constant risk climate change never exceed $1.48 bn.

The standard deviations reported in Table 11 give an indication of the uncertainty introduced by the use of 42 global climate models outputs to project climate change. This model uncertainty appears to be relatively constant across the four climate change scenarios, and is largest when it comes to future reservoir shares, followed by rainwater harvesting shares and desalination shares. Assuming constant risk in projected climate data eliminates between model uncertainty almost completely, with standard deviations across all assets and scenarios of between 0.00 and 0.03.

8. Conclusions

Changes in climatic conditions impact upon the risks and corisks of natural assets. To capture this time variation, a multivariate volatility model of water assets is specified based on augmenting the DCC conditional covariance model with realized volatility, referred to as RV DCC. The model was estimated by quasi maximum likelihood methods for two climate sensitive water assets, reservoir inflows, and rainwater harvesting. The empirical results were used to construct a dynamic portfolio of water supply, consisting of the two climate sensitive water assets, and desalinated water, which acted as a risk free asset as water from this source is independent of climatic conditions.

Implications of climate change on the water asset portfolio were investigated using econometric forecasting techniques based on historical data as well as by analyzing projected climate data for the two climate sensitive water assets. Econometric forecasting involved two bootstrapping schemes. In the first scheme, the RV DCC model was simulated over a 20-year horizon by sampling from the tails of the residual distribution to capture the effects of increased floods and droughts on the water portfolio. In the second scheme, the residuals were drawn from the residual distribution corresponding to a recent period, known as the Millennium Drought. To complement the simulation analysis, projected climate data for the same 20-year time horizon from up to 42 global climate models was obtained for four RCP scenarios and downscaled to generate flow projections for the two risky water assets.

The empirical results showed that reservoirs were on average the dominant source of water in the optimal portfolio during normal times, with minor contributions from rainwater harvesting and desalination. During extreme drought events, desalinated water had a relatively more important role in the portfolio, also coinciding with elevated contributions from rainwater harvesting. The results of the bootstrap experiments suggested that climate change necessitated portfolio rebalancing resulting in increased water supply costs of between 7% and 44% per year. Similar results were obtained from

TABLE 11. Simulated water portfolio results based on a 20-year forecast horizon using climate projection data for four scenarios. The number of climate models for each scenario are: 32 (RCP2.6), 42 (RCP4.5), 25 (RCP 6.0), and 39 (RCP8.5). Columns 3–5 report the average time varying shares computed from optimal monthly water portfolios based on equations (29) to (34), evaluated using the parameter values as per Table 6 and applying the RV DCC point estimates reported in columns 2 and 4 in Table 5 to the residuals of the climate projection data. Columns 6–8 report the optimal portfolio based on applying the constant risk point estimates reported in columns 6 and 8 of Table 5. *Desal Use* refers to the percentage of years in which desalination optimally contributes to the total cost-adjusted water stock. *Costs* report the average annual total supply cost of the optimal water portfolios.

		Asset Shares[a]					
		Time-Varying Risk			Constant Risk		
Scenario	Statistics	Reservoir	Rainwater	Desal.	Reservoir	Rainwater	Desal.
	Mean	0.64	0.32	0.04	0.93	0.07	0.00
	Median	0.72	0.28	0.00	0.94	0.06	0.00
RCP2.6	SD	0.27	0.21	0.10	0.02	0.02	0.00
	Desal. Use (% of yrs)			15.63			0.00
	Costs ($bn p.a.)			1.94			1.46
	Mean	0.75	0.22	0.03	0.93	0.07	0.00
	Median	0.85	0.15	0.00	0.94	0.06	0.00
RCP4.5	SD	0.22	0.14	0.10	0.03	0.02	0.02
	Desal. Use (% of yrs)			11.90			2.38
	Costs ($bn p.a.)			1.78			1.47
	Mean	0.54	0.37	0.09	0.93	0.07	0.00
	Median	0.63	0.37	0.00	0.93	0.07	0.00
RCP6.0	SD	0.34	0.24	0.13	0.02	0.02	0.00
	Desal. Use (% of yrs)			36.00			0.00
	Costs ($bn p.a.)			2.21			1.46
	Mean	0.69	0.27	0.04	0.92	0.08	0.00
	Median	0.79	0.21	0.00	0.93	0.07	0.00
RCP8.5	SD	0.25	0.18	0.09	0.03	0.02	0.01
	Desal. Use (% of yrs)			20.51			2.56
	Costs ($bn p.a.)			1.88			1.48

[a]Based on a desalination flow of $\mu_3 = 0.4$, and stocks of $S_1 = 0.65 \times 1290$ and $S_2 = 0.75 \times 0.217$, which represent the average stocks over the last 25 years of the data. A non-negativity restriction is imposed on some shares.

generating optimal portfolios based on projected climate data, with projected portfolio costs increasing by more than 30% under RCP6.0.

The proposed dynamic model of water assets builds on the existing literature of optimal water portfolios, by allowing for time varying conditional volatilities and co-volatilities, while preserving the advantage of analytical solutions. However, there are a number of ways the model can be expanded to capture additional dynamics linking the key variables within the model. One important extension of the theoretical model would be to include explicitly the multivariate GARCH volatility dynamics by speci-

fying an additional set of stochastic differential equations to capture time variations in the variances and covariances. The cost of this extension would be the need for numerical solutions to compute the portfolio shares as analytical solutions would no longer be available. Two methods for capturing the effects of climate change on future water portfolio were used, consisting of weighted bootstrapping methods to capture historical large movements in the water assets, and projected climate data generated from global climate models. An extension of these approaches would be to specify the moments of the stochastic differential equations to include climate change explicitly by making the moments functions of cumulative emissions. Finally, costs enter the model as deterministic variables. In a similar vein to the other proposed extensions, stochastic costs could be included by appending to the model stochastic differential equations capturing changes in costs over time. These extensions are left for future research.

References

ABS (2015), "Regional population growth, Australia 2014–15." Retrieved from http://www.abs.gov.au/AUSSTATS/abs@.nsf/mf/3218.0. [243]

Ahammed, F. (2017), "A review of water-sensitive urban design technologies and practices for sustainable stormwater management." *Sustainable Water Resources Management*, 3 (3), 269–282. [226]

Aït-Sahalia, Y. and J. Jacod (2014), *High-Frequency Financial Econometrics*. Princeton University Press. [230]

Andersen, T. G., T. Bollerslev, F. X. Diebold, and H. Ebens (2001), "The distribution of stock return volatility." *Journal of Financial Economics*, 61, 43–76. [230, 235]

Andersen, T. G., T. Bollerslev, F. X. Diebold, and P. Labys (2003), "Modeling and forecasting realized volatility." *Econometrica*, 71 (2), 579–625. [235]

Ando, A. W. and M. L. Mallory (2012), "Optimal portfolio design to reduce climate-related conservation uncertainty in the Prairie Pothole Region." *Proceedings of the National Academy of Sciences*, 109 (17), 6484–6489. [226]

Baillie, R. T. and R. J. Myers (1991), "Bivariate GARCH estimation of the optimal commodity futures hedge." *Journal of Applied Econometrics*, 6 (2), 109–124. [226]

Barndorff-Nielsen, O. E. and N. Shephard (2002), "Econometric analysis of realised volatility and its use in estimating stochastic volatility models." *Journal of the Royal Statistical Society B*, 64, 253–280. [230]

Bauwens, L., S. Laurent, and J. V. K. Rombouts (2006), "Multivariate GARCH models: A survey." *Journal of Applied Econometrics*, 21 (1), 79–109. [226]

Bollerslev, T. (1986), "Generalized autoregressive conditional heteroskedasticity." *Journal of Econometrics*, 31 (3), 307–327. [232]

Bollerslev, T., N. Meddahi, and S. Nyawa (2019), "High-dimensional multivariate realized volatility estimation." *Journal of Econometrics*, 210, 116–136. [234]

Bollerslev, T., A. J. Patton, and R. Quaedvlieg (2020), "Multivariate leverage effects and realized semicovariance GARCH models." *Journal of Econometrics*, 217 (2), 411–430. [234]

Brownlees, C. and R. F. Engle (2016), "SRISK: A conditional capital shortfall measure of systemic risk." *Review of Financial Studies*, 30, 48–79. [249]

Duran Vinent, O., R. J. Johnston, M. L. Kirwan, A. D. Leroux, and V. L. Martin (2019), "Coastal dynamics and adaptation to uncertain sea level rise: Optimal portfolios for salt marsh migration." *Journal of Environmental Economics and Management*, 98, 102262. [226]

Engle, R. and A. Patton (2001), "What is a good volatility model?" *Quantitative Finance*, 1, 237–245. [240]

Engle, R. F. (1982), "Autoregressive conditional heteroskedasticity with estimates of the variance of United Kingdom inflation." *Econometrica*, 50, 987–1008. [230, 232]

Engle, R. F. (2002), "Dynamic conditional correlation: A simple class of multivariate generalized autoregressive conditional heteroskedasticity models." *Journal of Business & Economic Statistics*, 20 (3), 339–350. [226, 232, 234, 235, 236]

Glosten, L. R., R. Jagannathan, and D. E. Runkle (1993), "On the relation between the expected value and the volatility of the nominal excess return on stocks." *Journal of Finance*, 48, 1779–1801. [240]

Hansen, P. R., Z. Huang, and H. H. Shek (2012), "Realized GARCH: A joint model for returns and realized measures of volatility." *Journal of Applied Econometrics*, 27, 877–906. [234]

Hansen, P. R., A. Lunde, and V. Voev (2012), "Realized beta GARCH: A multivariate GARCH model with realized measures of volatility." *Journal of Applied Econometrics*, 29, 774–799. [226, 232, 233, 235, 240]

Humphreys, H. B. and K. T. McClain (1998), "Reducing the impacts of energy price volatility through dynamic portfolio selection." *The Energy Journal*, 19 (3), 107–131. [225, 226, 242]

Leroux, A. D., V. L. Martin, and K. A. St. John (2022), "Supplement to 'Modeling time varying risk of natural resource assets: Implications of climate change'." *Quantitative Economics Supplemental Material*, 13, https://doi.org/10.3982/QE1597. [241]

Leroux, A. D. and V. L. Martin (2016), "Hedging supply risks: An optimal water portfolio." *American Journal of Agricultural Economics*, 98 (1), 276–296. [225, 241, 243, 245, 247]

Leroux, A. D., V. L. Martin, and H. Zheng (2018), "Addressing water shortages by force of habit." *Resource and Energy Economics*, 53, 42–61. [226, 242]

Mallory, M. L. and A. W. Ando (2014), "Implementing efficient conservation portfolio design." *Resource and Energy Economics*, 38, 1–18. [226]

Martin, V. L., S. Hurn, and D. Harris (2013), *Econometric Modelling With Time Series: Specification, Estimation and Testing*. Cambridge University Press, Cambridge, U.K. [236]

Melbourne Water (2013), "Melbourne water 2013 water plan." Melbourne Water, Melbourne, Australia. [243]

Melbourne Water (2018), "Water storage and use." URL: https://www.melbournewater.com.au/water/water-storage-and-use#/, accessed 28 May 2018. [244]

Merton, R. C. (1969), "Lifetime portfolio selection under uncertainty: The continuous-time case." *Review of Economics and Statistics*, 51 (3), 247–257. [225, 226]

Merton, R. C. (1971), "Optimum consumption and portfolio rules in a continuous-time model." *Journal of Economic Theory*, 3 (4), 373–413. [226]

Peel, M., R. Srikanthan, T. McMahon, and D. Karoly (2015), "Approximating uncertainty of annual runoff and reservoir yield using stochastic replicates of global climate model data." *Hydrology and Earth System Sciences*, 19 (4), 1615–1639. [252]

Raupach, M. R., P. R. Briggs, V. Haverd, E. A. King, M. Paget, and C. M. Trudinger (2009), "Australian water availability project (AWAP). CSIRO marine and atmospheric research component: Final report for phase 3." CAWCR Technical Report No. 013. 67 pp. [227]

Raupach, M. R., P. R. Briggs, V. Haverd, E. A. King, M. Paget, and C. M. Trudinger (2012), "Australian water availability project." CSIRO Marine and Atmospheric Research, Canberra, Australia, http://www.csiro.au/awap. [227]

Sanchirico, J. N., M. D. Smith, and D. W. Lipton (2008), "An empirical approach to ecosystem-based fishery management." *Ecological Economics*, 64 (3), 586–596. [226]

Shah, P. and A. W. Ando (2015), "Downside versus symmetric measures of uncertainty in natural resource portfolio design to manage climate change uncertainty." *Land Economics*, 91 (4), 664–687. [226]

Stocker, T. F., D. Qin, G. K. Plattner, M. M. Tignor, S. K. Allen, J. Boschung, A. Nauels, Y. Xia, V. Bex, and P. M. Midgley (2014), "Climate change 2013: The physical science basis." Contribution of working group I to the fifth assessment report of IPCC the intergovernmental panel on climate change. Cambridge, U.K. and New York, USA. [226, 249, 252]

Tischbirek, A. (2019), "Long-term government debt and household portfolio composition." *Quantitative Economics*, 10 (3), 1109–1151. [226]

WWAP (2012), "The United Nations world water development report 4: Managing water under uncertainty and risk." World Water Assessment Programme, UNESCO, Paris. [226]

Co-editor Tao Zha handled this manuscript.

Manuscript received 7 April, 2020; final version accepted 10 July, 2021; available online 28 July, 2021.